Current Topics in Peptide & Protein Research
Vol. 17, 2016

Original Communication

Degradation of human lung elastin matrix

Jiangtao He[a], Shuren Ma[a], Jerome Cantor[b], Toyonobu Usuki[c], Georgia Dolios[d], Rong Wang[d], Gerard M. Turino[a] and Yong Y. Lin[a,*]

[a]Department of Medicine, St. Luke's-Roosevelt at Mount Sinai, NY, USA;
[b]School of Pharmacy and Allied Health Sciences, St. John's University, NY, USA.
[c]Department of Materials and Life Sciences, Sophia University, Tokyo, Japan.
[d]Department of Genetics and Genomic Science, Icahn School of Medicine at Mount Sinai, NY, USA.

ABSTRACT

Elastin matrix are significant structural constituents of skin, blood vessels, lung, and other connective tissues, where they provide physical recoil to distorting forces and contribute to normal physiological function. Degradation of elastin-containing tissues can occur in prevalent diseases resulting in complex mixtures of elastin-derived peptides, which remain largely uncharacterized due to the insoluble nature of elastin and its complex crosslinking structure. We compared proteolytic activity of several proteinases that cause degradation of human lung elastin matrix. The resulting peptides were characterized by high performance liquid chromatography and tandem mass spectrometry (LC-MS/MS), which results in the identification of several hundreds of linear peptides that belong to non-crosslinking domains of soluble elastin precursor tropoelastin. The analysis of the proteolytically cleaved sites of tropoelastin domains suggested that two alanine-rich lysine peptide chains at the domains 19 and 25 of tropoelastin are involved in the crosslink formation and it is proposed that a tetrafunctional crosslink structure is formed by condensation between the two domains, KAAAK (K at the loci 375 and 379) and KSAAK (K at the loci 529 and 533) of tropoelastin. The proposed crosslink can be chemically synthesized as a molecular model for the elastin crosslinking structure. We further compared *in vitro* proteolysis of a normal lung and a lung from a chronic obstructive pulmonary disease (COPD) patient. The proteolysis showed the three proteases HNE, MMP12 and PR3 are the most effective toward elastin matrix degradation, which may also occur *in vivo* during COPD. The proteolysis of the COPD lung produced decreased amount of desmosine/isodesmosine (DES/IDS) crosslink peptides compared to that of the normal lung but involved more proteolytic sites, which indicated significant pathological degradation of the crosslinks had occurred within the elastin matrix of the COPD lung resulting in an altered structural integrity. This finding could be a basis for progression of lung tissue breakdown once COPD is initiated and be a mechanism for clinical progression of COPD.

KEYWORDS: elastin, elastin peptides, crosslink structure, COPD

INTRODUCTION

Elastic fibers of extracellular matrix (ECM) are significant structural constituents of skin, blood vessels, lung, and other connective tissues, where they provide physical recoil to distorting forces and contribute to normal physiological function. Degradation of elastin-containing tissues can occur in prevalent diseases, where elastin can be degraded into soluble peptide fragments by the elastolytic enzymes from neutrophils and macrophages [1, 2]. Lung elastin degradation occurs with the development of pulmonary emphysema in patients with chronic obstructive pulmonary disease (COPD). The disease

*Corresponding author: yylin@chpnet.org

is characterized by destruction of alveolar walls, obstruction of bronchioles, and trapping of air. The disease develops mainly from exposure to tobacco smoke or inherited alpha-1 antitrypsin deficiency [3-5].

Elastin, a major structural component of elastic fibers, is a highly crosslinked insoluble protein formed by posttranslational modification of lysine residues in the soluble precursor, tropoelastin (792 amino acids) by lysyl oxidase and condensation reactions. Desmosine (DES) and isodesmosine (IDS) are two tetrafunctional pyridinium amino acids that serve as major crosslinking molecules binding the polymeric chains of amino acids into the 3D network of elastin [6-8]. We have developed an isotope dilution tandem mass spectrometric (LC-MS/MS) analysis that utilizes an acid stable internal standard desmosine-d_4, synthesized in our laboratory [9, 10]. The method allows accurate and sensitive measurements of DES and IDS to study the degradation of elastin crosslinks involved in biological systems [10] and has been effectively applied to measure DES and IDS in urine, plasma, sputum, and bronchoalveolar lavage fluid (BALF) as biomarkers for elastin degradations involved in COPD or secondhand smoke exposure [11-16].

Elevated biomarker DES/IDS levels in COPD patients reflect increased pulmonary elastin breakdown that produces elastin-derived peptides (EDPs). There is evidence that EDPs induce some significant biological activities such as chemotaxis and antigenicity [17-21], but their molecular structure relationship remains uninvestigated [22]. In this report, we investigated the elastin degradation *in situ* of lung extracellular matrix (ECM) in human COPD to study its degradation of crosslinked structure and to identify the peptides from such degradation. Inflammatory cell proteinases are believed to be responsible for destruction of alveolar matrix in emphysema. Various proteinases, such as serine proteinases, cysteine proteinases and metalloproteinases (MMPs), present in respiratory bronchioles have been reported to involve in the pathogenesis of COPD [23]. To study the possible pathogenic effect of these proteolytic enzymes, we compared the *in vitro* proteolytic activity of the seven enzymes causing degradation of lung elastin matrix. The resulting peptide fragments were analyzed for the contents of DES and IDS to examine the degradation of elastin crosslinks. Peptide fragments were studied for their amino acid sequences by proteomic LC-MS/MS analysis to ascertain whether the COPD lung exposed to proteases produces a detectable different profile of peptides than normal lung.

MATERIALS AND METHODS

Materials

Desmosine and isodesmosine were products of Elastin Products Company (Owensville, MS) and the acid stable desmosine-d_4 was chemically synthesized in our laboratory [9, 10]. Proteolytic enzymes used were human neutrophil elastase (HNE) from Elastin Products Co. Metalloproteinases (MMP12, MMP9, MMP8 and MMP2) and Proteinase-3 (PR3) were from Enzo Life Science (Farmingdale, NY).

Lung elastin matrix

Autopsy tissues from a normal and an emphysematous lung were obtained from the Department of Pathology, Hospital and Medical Center, Brookdale University, New York. The samples were dissected free of major airways and blood vessels, washed to remove blood, then homogenized in distilled water. Following lyophilization, the tissues were suspended in 1 M NaCl (50 mL) for 24 hr and centrifuged. The supernatant was discarded after centrifugation, and then the pellet was resuspended in 1 M NaCl. This extraction process was repeated three times, and the insoluble residue was washed with distilled water. After centrifugation the insoluble residue was defatted with chloroform/methanol (2:1, v/v) for 48 hr, consecutively washed with water and ethanol, and dried in vacuum under P_2O_5 in preparation for proteolytic digestion.

Proteolytic digestion

Lung elastin matrix samples (1 mg) were suspended in 0.8 mL of Tris buffer (Tris 50 mM, 200 mM NaCl, 10 mM $CaCl_2$, pH = 7.5) and sonicated for 10 min. The digestion was initiated by addition of 0.1 mL of proteolytic enzyme (5 μg in Tris buffer) at 37 °C for 24 hr, and continued for another 24 hr with a second addition of 0.1 mL enzyme solution. The digestion was stopped by addition of 20 μL of 1 mg/mL protease inhibitor cocktail (Sigma P-2714). The resulting mixture was centrifuged at 3000 rpm for 10 minutes to separate the undigested ECM solid. The supernatant was separated into different

molecular weight fractions by membrane filtration using Ultrafilter (Millipore) and stored at -20 °C for LC-MS/MS analysis.

Quantitation of DES and IDS by the LC-MS/MS analysis

Quantitation of DES and IDS in the enzyme digests were carried out by the isotope dilution LC-MS/MS analysis we have previously developed [10]. Briefly, it consists of three steps as follows: Step 1 - Acid hydrolysis: Desmosine-d_4 internal standard (IS, 5 ng) was added to the analytical samples (1 mL) in a glass vial with equal volumes of conc. HCl (37%). Air in the vial was displaced with nitrogen, and was heated at 110 °C for 24 hr. The hydrolyzed sample was filtered and evaporated to dryness. Step 2 - Cellulose (CF1) cartridge extraction: The acid hydrolyzed samples (after drying under vacuum or nitrogen stream to remove residual acid) were dissolved in 2 mL of n-butanol/acetic acid/water (4:1:1), and applied onto a 3 mL cellulose cartridge. The cartridge was prepared by the introduction of 3 mL of 5% CF1 cellulose powder in n-butanol/acetic acid/water (4:1:1) and stirring for 24 hr to form a well dispersed slurry. The cartridge was washed 3 times with 3 mL of n-butanol/acetic acid/water (4:1:1), and the samples retained in the cartridge were eluted with 3 mL of water, dried and dissolved in 100 µL of LC mobile phase and analyzed by LC-MS/MS. Step 3 - LC-MS/MS analysis: A TSQ Discovery electrospray tandem mass spectrometer (Thermo Scientific, San Jose, CA) was used for LC-MS/MS analysis. HPLC conditions used were a 2 mm × 150 mm dC18 (3 µm) column (Waters, MA) and the mobile phase A (7 mM HFBA/5 mM NH_4Ac in water) and B (7 mM HFBA/5 mM NH_4Ac in 80% acetonitrile) were programmed linearly from 100% A to 82% A in 12 min. Quantitation was performed by selected reaction monitoring (SRM) of the transitions of both DES and IDS (m/z 526 to m/z 481 + m/z 397) and the internal standard (m/z 530 to m/z 485), with collision energy set at 33 V for both transitions, collision gas pressure at 1.5 m Torr, tube lens at 132 V, with sheath gas pressure set at 45 and auxiliary gas pressure at 6 units and ion spray voltage at 3.8 kV. The scan time was set at 1.00 ms and both quadrupoles (Q1 and Q3) were at 0.7 Da FWHM.

Characterization of peptides by LC-MS/MS analysis

Peptides with molecular weight below 10 kD produced by the enzymatic digests were characterized by tandem mass spectrometric analysis using an online LC-MS/MS system consisting of a Water NanoAcquity UPLC (Waters, Milford, MA) and a LTQ-Orbitrap mass spectrometer (Thermo Scientific, San Jose, CA). The peptides were reconstituted with 0.1% formic acid in acetonitrile (ACN) and water (2:98, v/v) and injected into a Symmetry® C18 (180 µm x 100 mm, 5 µm particle size) trap column (Waters, Milford) prior to the separation on a BEH130 C18 (75 µm x 150 mm, 1.7 µm particle size) reversed-phase column (Waters, Milford, MA). Peptides were eluted using a gradient of 0.1% formic acid in water as solvent A and 0.1% formic acid in ACN as solvent B, with solvent B raised from 5 to 30% in 60 minutes, then 30 to 85% in the next 10 min at a flow rate of 0.3 µL/minute. The mass spectrometer was operated in the positive ion mode with a spray voltage of 1.2 kV, ion transfer tube voltage of 40 V and ion transfer tube temperature of 150 °C. A normalized collision energy of 35% and activation time of 30 ms were applied in MS/MS acquisitions. The top eight most intense ions were selected for fragmentation in the LTQ and the mass range selected was from m/z 300-2000. Dynamic exclusion was used with repeat count of 1, repeat duration of 30 s and exclusion duration of 60 s. MS/MS spectra were searched against *Uniprot Homo sapiens* proteomic dataset using Mascot and X! Tandem as search engines with a non-specific digestion enzyme. The search was performed using a parent ion tolerance of 5.0 ppm and with a fragment ion mass tolerance of 0.60 Da; oxidized methionine, histidine and tryptophan (+15.9949 Da), deamidated asparagine and glutamine (+0.9840 Da), were specified as differential modifications. Scaffold (version Scaffold_4.5.3, Proteome Software Inc., Portland, OR) was used to validate MS/MS-based peptide and protein identifications.

RESULTS

Degradation of elastin crosslinks

Two serine proteases, human neutrophil elastase (HNE) and proteinase 3 (PR3), and four metalloproteinases, MMP2, MMP8, MMP9 and MMP12, were compared for their *in vitro* proteolytic activity toward human lung elastin matrix. The *in vitro* enzymatic digestions of elastin from a normal and an emphysematous COPD lung elastin matrix were carried out at 37 °C. The peptides formed by the digestions were fractionated into five molecular weight fractions: 1) below 10 kD, 2) 10 kD to 50 kD,

3) 50 kD to 100 kD, 4) above 100 kD, and 5) undigested residual solids. Each peptide fraction was acid hydrolyzed and DES and IDS were measured by the isotope dilution LC-MS/MS analysis [10], which represents the amounts of the elastin crosslinks degraded into the peptide fractions. The DES and IDS measurements in each peptide fractions obtained from the proteolytic digestions are summarized in fig. 1. The three proteases HNE, PR3, and MMP12 were much more effective in the degradation of the elastin crosslinks than the other three proteases MMP 9, 8 and 2. HNE is the most effective which degrades approximately 50% of the crosslinks in the normal lung; MMP12 and PR3 are also effective in degrading 44% and 32% of the crosslinks, respectively. The three other proteases MMP9, 8, and 2 are nearly inactive toward the degradation of lung elastin matrix where elastin remains as undigested solid (results not shown). The largest proportion of the DES and IDS crosslinked peptides are identified in the peptide fractions of molecular weights between 10 kD to 50 kD. We also conducted *in vitro* proteolytic digestion of lung ECM obtained from a COPD patient with emphysema. The three proteases HNE, MMP12 and PR3 were the most effective in the elastic matrix degradation, but less amounts of DES and IDS crosslinked peptides resulted from the digestion. HNE degrades only 32%, PR3 degrades 26%, and MMP12 degrades 9% of the crosslinks. Most abundant crosslinks were also found in the peptide fraction 2 of molecular weights between 10 kD to 50 kD.

LC-MS/MS characterization of peptide fragments

The electrospray mass spectrometry study shows that abundant mass spectrometric ions are produced by the peptide fractions below 10 kD, but not with those peptide fractions between 10–50 kD. This may be due to the possibility that such high molecular weight peptides are difficult to fragment under the ion-trap condition. Thus the peptide fractions below

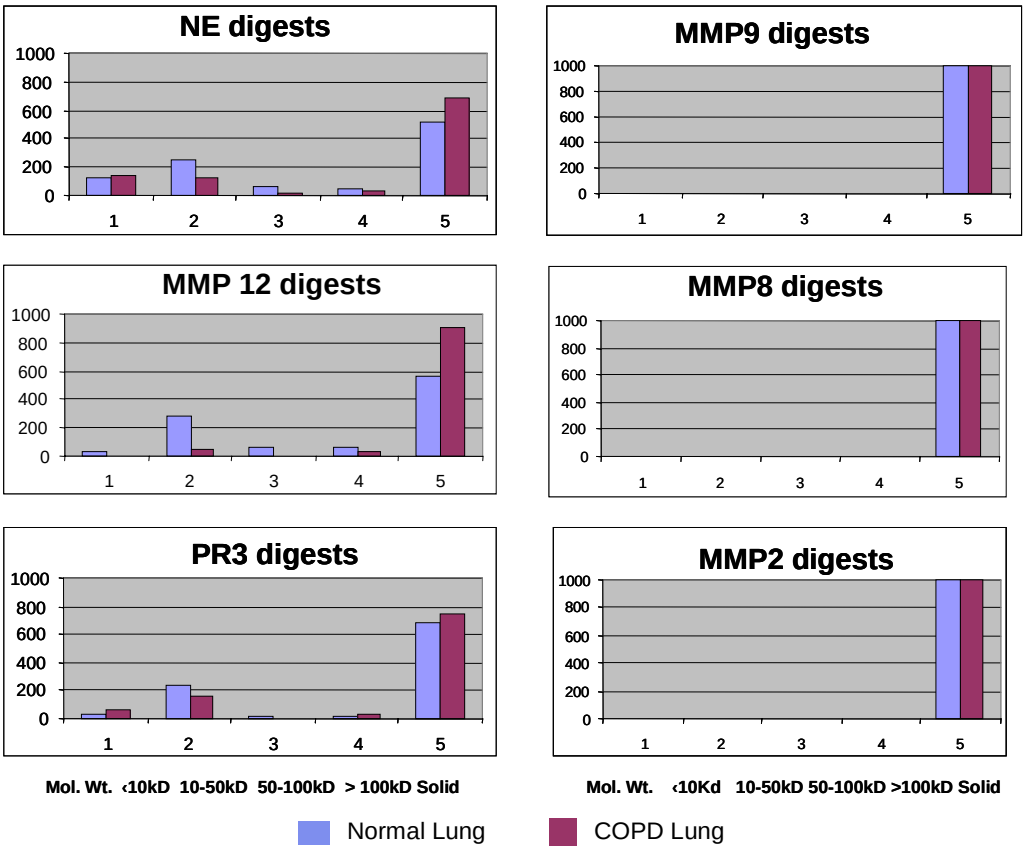

Fig. 1. Distributions of DES/IDS peptides obtained from the proteolytic digests of normal lung (1,000 ug) and COPD lung (1,000 ug).

10 kD which have been effectively degraded from lung elastic tissue by the three proteolytic enzymes (HNE, MMP12, and PR3) were studied for their peptide characterization (amino acid sequences) by LC-MS/MS analysis that searches their MS/MS spectra against the protein database.

The proteomic analysis of the normal lung ECM identified large numbers of the linear peptides: 49 from the HNE, 171 from the MMP12, and 115 peptides from the PR3 digestions. The identities of peptides are shown in table 1a, 1b and 1c.

Table 1a. 49 peptides from NE digestion of normal lung ECM (<10 kD).

No	Peptides	Location
1	FYPGAGLGAL	42-51
2	FYPGAGLGALGGGA	42-55
3	KPVPGGLAGA	64-73
4	GLAGAGLGA	69-77
5	GLGAGLGAFPA	74-84
6	GLGAGLGAFPAV	74-85
7	GLGAFPAVTFPG	78-89
8	LVPGGVADAAA	91-101
9	KAGAGLGGVPGVGGLGV	107-123
10	GLGGVPGVGGLGV	111-123
11	GVLPGARFPGV	153-163
12	VGVLPGVPT	163-171
13	GIPGVGPFGGPQPGVPL	188-204
14	GKLPYGYGPGGV	224-235
15	AGLVPGGPGFGPGV	320-333
16	GLVPGGPGFGPGV	321-333
17	GLVPGGPGFGPGVV	321-334
18	LVPGGPGFGPGVV	322-334
19	GVPGAGVPGVGVPG	335-348
20	VPGAGIPGAAVPGVV	354-368
21	AVPGVVSPEAA	363-373
22	KYGARPGVGV	382-391
23	VGVGGIPT	389-396
24	GGFPGFGV	402-409
25	GGFPGFGVGV	402-411
26	GLVPGVGVAPGVGV	469-485
27	QFGLVPGVGV	470-479
28	QFGLVPGVGVAPGVGV	470-485

Table 1a continued..

29	QFGLVPGVGVAPGVGVAPGVGV	470-491
30	FGLVPGVGV	471-479
31	GLAPGVGVAPGVGV	496-509
32	APGIGPGGVAAA	516-527
33	AGLGAGIPGLGV	544-555
34	AGLGAGIPGLGVGV	544-557
35	GVPGLGVGAGVPGLGV	558-573
36	GAGVPGLGVGAGVPGFGAVPG	565-585
37	GAGVPGFG	574-581
38	AAVPGVLGGLGAL	597-609
39	AVPGVLGGLGAL	598-609
40	AVPGVLGGLGALGGV	598-612
41	VPGVLGGLGAL	599-609
42	VPGVLGGLGALGGV	599-612
43	PGVLGGLGALGGV	600-612
44	VLGGLGALGGV	602-612
45	GGLGALGGVGIPGGVV	604-619
46	AGLGGVLGGAGQFPL	680-684
47	GLGGVLGGAGQFPL	681-694
48	LGGAGQFPLGGV	686-697
49	AARPGFGLSPI	698-708

Table 1b. 171 peptides from MMP12 digestion of normal lung ECM (<10 kD).

No	Peptides	Location
1	VFYPGAGLGA	41-50
2	GGGALGPGGKPLKP	52-65
3	LAGAGLGAGLGAFP	70-83
4	LAGAGLGAGLGAFPAVTFPGA	70-90
5	AGAGLGAGLGAFP	71-83
6	AGAGLGAGLGAFPAVTFPGA	71-90
7	LGAGLGAFPAVTFPGA	75-90
8	AFPAVTFPGA	81-90
9	ALVPGGVADAAAA	90-102
10	LVPGGVADAAAA	91-102
11	AKAGAGLGGVPGVGGLG	106-122
12	AGAGLGGVPGVGG	108-120
13	AGAGLGGVPGVGGLG	108-122

Table 1b continued..

14	GAGLGGVPGVGGLG	109-122
15	AGLGGVPGVGG	110-120
16	AGLGGVPGVGGLG	110-122
17	GGVPGVGGLG	113-122
18	VGLPGVYPGGVLP	144-156
19	GLPGVYPGGVLP	145-156
20	GLPGVYPGGVLPG	145-157
21	VYPGGVLPGARFPG	149-162
22	VYPGGVLPGARFPGVG	149-164
23	VYPGGVLPGARFPGVGVLPGVPTG	149-172
24	GGVLPGARFPGVGVLPGVPTG	152-172
25	GVLPGARFPGVGVLPGVPTG	153-172
26	VLPGARFPGVGVLPGVPTG	154-172
27	GARFPGVGVLPGVP	157-170
28	GARFPGVGVLPGVPT	157-171
29	GARFPGVGVLPGVPTG	157-172
30	GARFPGVGVLPGVPTGA	157-173
31	GARFPGVGVLPGVPTGAG	157-174
32	ARFPGVGVLPGVPT	158-171
33	ARFPGVGVLPGVPTG	158-172
34	ARFPGVGVLPGVPTGA	158-173
35	ARFPGVGVLPGVPTGAG	158-174
36	FPGVGVLPGVPT	160-171
37	FPGVGVLPGVPTG	160-172
38	PGVGVLPGVPTG	161-172
39	GVGVLPGVPTG	162-172
40	VGVLPGVPT	163-171
41	VGVLPGVPTGA	163-173
42	VGVLPGVPTGAGVKPK	163-178
43	FAGIPGVGPF	186-195
44	IPGVGPFG	189-196
45	FGGPQPGVPLGYP	195-207
46	YGPGGVAGAAGKAGYPTG	230-247
47	YGPGGVAGAAGKAGYPTGTGVGPQA	230-254
48	FGAGAAGVLPGVGG	266-279
49	FGAGAAGVLPGVGGAG	266-281

Table 1b continued..

50	FGAGAAGVLPGVGGAGVPGVPGA	266-288
51	FGAGAAGVLPGVGGAGVPGVPGAIPGIGG	266-294
52	AGAAGVLPGVGGAG	268-281
53	GAAGVLPGVGGAG	269-281
54	AAGVLPGVGGAGVPGVPGA	270-288
55	AGVLPGVGGAG	271-281
56	AGVLPGVGGAGVPGVPGA	271-288
57	GVLPGVGGAGVPGVPGA	272-288
58	VLPGVGGAGVPGVPGA	273-288
59	AGVPGVPGAIPGIGG	280-294
60	VPGVPGAIPGIGG	282-294
61	IPGIGGIAG	289-297
62	AGLVPGGPGF	320-329
63	LVPGGPGFGPGV	322-333
64	LVPGGPGFGPGVVG	322-335
65	LVPGGPGFGPGVVGVPGAGVPGVG	322-345
66	LVPGGPGFGPGVVGVPGAGVPGVGVPGAG	322-350
67	VPGGPGFGPGVVG	323-335
68	FGPGVVGVPGAG	329-340
69	FGPGVVGVPGAGVPG	329-343
70	FGPGVVGVPGAGVPGVG	329-345
71	FGPGVVGVPGAGVPGVGVPGAGIP	329-352
72	GPGVVGVPGAGVPG	330-343
73	GPGVVGVPGAGVPGVG	330-335
74	GPGVVGVPGAGVPGVGVPG	330348
75	GPGVVGVPGAGVPGVGVPGAG	330-350
76	GPGVVGVPGAGVPGVGVPGAGIPVVPGAG	350-358
77	VVGVPGAGVPGVG	333-345
78	VVGVPGAGVPGVGVPG	333-348
79	VVGVPGAGVPGVGVPGAG	333-350
80	VGVPGAGVPGVG	334-345
81	VGVPGAGVPGVGVPGAG	334-450

Table 1b continued..

82	GVPGAGVPGVGVPGAG	335-350
83	VPGAGVPGVGVPGAG	356-350
84	GAGVPGVGVPGAG	338-350
85	AGVPGVGVPGAG	339-350
86	VPGVGVPGAGIPVVPG	341-356
87	IPVVPGAGIPGA	351-262
88	IPVVPGAGIPGAA	351-363
89	IPVVPGAGIPGAAVPGVVSPEA	351-372
90	VPGVVSPEA	364-372
91	VPGVVSPEAAA	364-374
92	YGARPGVGVGGIPT	383-396
93	YGARPGVGVGGIPTY	383-397
94	YGARPGVGVGGIPTYGVG	383-400
95	GARPGVGVGGIPTYG	384-398
96	ARPGVGVGGIPTYG	385-398
97	GVGVGGIPTYG	388-398
98	GVGVGGIPTYGVG	388-400
99	VGAGGFPGFG	399-408
100	GAGGFPGFGVG	400-410
101	FGVGVGGIPGVAG	407-419
102	FGVGVGGIPGVAGVPGVGGVPGVGGVPG	407-434
103	FGVGVGGIPGVAGVPGVGGVPGVGGVPGVGI	407-437
104	VGGIPGVAGVPGV	411-423
105	VAGVPGVGGVPGVGGVPG	417-434
106	AGVPGVGGVPGVGG	418-431
107	AGVPGVGGVPGVGGVPG	418-434
108	AGVPGVGGVPGVGGVPGVG	418-436
109	AGVPGVGGVPGVGGVPGVGI	418-437
110	AGVPGVGGVPGVGGVPGVGISPEA	417-441
111	VPGVGGVPGVGGVPG	420-434
112	VPGVGGVPGVGGVPGVG	420-435
113	VPGVGGVPGVGGVPGVGI	420-437
114	GVGGVPGVGGVPG	422-434
115	GVGGVPGVGGVPGVGI	422-437
116	VGGVPGVGGVPG	423-434

Table 1b continued..

117	VGGVPGVGGVPGVG	423-436
118	VGGVPGVGGVPGVGI	423-437
119	VGGVPGVGGVPGVGISPEA	423-441
120	GGVPGVGGVPGVG	424-436
121	GGVPGVGGVPGVGI	424-437
122	VPGVGGVPGVGI	426-437
123	VPGVGGVPGVGISPEA	426-441
124	PGVGGVPGVGI	427-437
125	GVGGVPGVGISPEA	428-441
126	VPGVGISPEA	432-441
127	FGLVPGVGVAPGVGVAPGVGVAPGVG	471-496
128	FGLVPGVGVAPGVGVAPGVGVAPGVGL	471-497
129	GLVPGVGVAPGVGVAPGVGVAPGVGL	472-497
130	LVPGVGVAPGVG	475-484
131	VGVAPGVGVAPGVG	477-490
132	VGVAPGVGVAPGVGV	477-491
133	GVAPGVGVAPGVG	478-490
134	GVAPGVGVAPGVGVAPG	478-494
135	GVAPGVGVAPGVGVAPGVG	478-496
136	GVAPGVGVAPGVGVAPGVGL	478-497
137	VAPGVGVAPGVGV	479-491
138	APGVGVAPGVGVAPG	480-494
139	VGVAPGVGVAPGVGL	483-497
140	GVAPGVGVAPGVGL	484-497
141	VAPGVGVAPGVGL	485-497
142	GLAPGVGVAPGVGVAPG	496-512
143	GVAPGVGVAPGVGVAPGIGPGG	502-523
144	VGVAPGVGVAPGIGPGG	507-523
145	GVAPGVGVAPGIGPGG	508-523
146	VAPGVGVAPGIGPGG	509-523
147	APGVGVAPGIGPGG	510-523
148	GVGVAPGIGPGG	512-523
149	VGVAPGIGPGGVA	513-525
150	GAGIPGLGVGVGVPGL	547-562
151	GAGIPGLGVGVGVPGLG	547-563

Table 1b continued..

152	GAGIPGLGVGVGVPGLGVGAG	547-567
153	PGLGVGVGVPG	551-561
154	GLGVGVGVPGLG	552-563
155	LGVGVGVPGLG	553-563
156	GVGVGVPGLGVGAGVPG	554-570
157	GVGAGVPGLGVGAG	563-576
158	GVGAGVPGLGVGAGVPG	563-579
159	LGVGAGVPGFGA	571-582
160	GVGAGVPGFGA	572-582
161	VPGVLGGLGA	599-608
162	GALGGVGIPGG	607-617
163	VGAAGLGGLGVGG	642-654
164	GLGGLGVGGLG	646-656
165	GVGGLGVPGVGG	651-662
166	GVPGVGGLGG	656-665
167	LGGVLGGAGQFPLG	682-695
168	GGVLGGAGQFP	683--693
169	GGVLGGAGQFPLG	683-695
170	GGVLGGAGQFPLGG	683-696
171	GGVAARPGFGL	695-705

Table 1c. 115 peptides from PR3 digestion of normal lung ECM (<10 kD).

No	**Peptides**	**Location**
1	FYPGAGLGAL	42-51
2	LGGGALGPGGKPLKPVPGGL	51-70
3	LGGGALGPGGKPLKPVPGGLA	51-71
4	LGGGALGPGGKPLKPVPGGLAGA	51-73
5	LGGGALGPGGKPLKPVPGGLAGAGLGA	51-77
6	GLGAGLGAFPAV	74-85
7	VTFPGALVPGGV	85-96
8	VTFPGALVPGGVADAA	85-100
9	KAGAGLGGVPGVGGLGV	107-123
10	GAGLGGVPGVGGLGV	109-123
11	ARFPGVGVLPGVPT	158-171

Table 1c continued..

12	ARFPGVGVLPGVPTG	158-172
13	RFPGVGVLPGVPT	159-171
14	GAGVKPKAPGVGGA	172-185
15	AGIPGVGPFGGPQPGVPL	187-204
16	GIPGVGPFGGPQPGVPL	188-204
17	KAPKLPGGY	209-217
18	GLPYTTGKLPY	218-228
19	GYGPGGVAGA	229-238
20	GYGPGGVAGAAGKA	229-242
21	AGVLPGVGGAGVPGVPGAIPG	271-291
22	GVLPGVGGAGVPGVPGAIPGIG	272-293
23	GGAGVPGVPGAIPGIGGIAGVGTPA	278-302
24	AIPGIGGIAGVGTPA	288-302
25	GLVPGGPGFGPGVVGVPGAGVPGV	321-344
26	VVGVPGAGVPGVGVPGAGIPV	333-353
27	VGVPGAGVPGVGVPGAGIPV	334-353
28	VGVPGAGVPGVGVPGAGIPVVPGA	334-357
29	GVPGAGVPGVGVPGAGIPV	335-353
30	GVPGAGVPGVGVPGAGIPVVPG	335-356
31	GVPGAGVPGVGVPGAGIPVVPGA	335-357
32	AGVPGVGVPGAGIPVVPGAGIPG	339-361
33	AGVPGVGVPGAGIPVVPGAGIPGAAVPGVV	339-368
34	VGVPGAGIPVVPGAGIPGAAVPGV	344-367
35	VPGAGIPGAAVPGVVSPEAA	354-373
36	GARPGVGV	384-391
37	GARPGVGVGGIPTYGV	384-399
38	AGVPGVGGVPGVGGVPGVGISPEAQ	418-442
39	GVPGVGGVPGVGGVPGVGISPEAQ	419-442
40	VGGVPGVGGVPGVGISPEA	423-441
41	VGGVPGVGGVPGVGISPEAQ	423-442

Table 1c continued..

42	GGVPGVGGVPGVGISPEAQ	424-442
43	AQFGLVPGVGVAPGVGVAPGV	469-489
44	AQFGLVPGVGVAPGVGVAPGVGVAPGV	469-495
45	QFGLVPGVGVAPGVGV	470-485
46	QFGLVPGVGVAPGVGVAPGV	470-489
47	QFGLVPGVGVAPGVGVAPGVG	470-490
48	QFGLVPGVGVAPGVGVAPGVGV	470-491
49	QFGLVPGVGVAPGVGVAPGVGVAPGV	470-495
50	GLVPGVGVAPGV	472-483
51	GLVPGVGVAPGVGVAPG	472-488
52	GLVPGVGVAPGVGVAPGVGVAPGV	472-495
53	LVPGVGVAPGVGVAPGVGVAPGV	473-495
54	VGVAPGVGVAPGVGVAPGV	477-495
55	GVAPGVGVAPGVGVAPGV	478-495
56	GLAPGVGVAPGVGVAPGV	496-513
57	GLAPGVGVAPGVGVAPGVGV	496-515
58	GLAPGVGVAPGVGVAPGVGVAPG	496-518
59	GLAPGVGVAPGVGVAPGVGVAPGIG	496-520
60	GLAPGVGVAPGVGVAPGVGVAPGIGPG	496-522
61	GLAPGVGVAPGVGVAPGVGVAPGIGPGGV	496-524
62	GLAPGVGVAPGVGVAPGVGVAPGIGPGGVA	496-525
63	GLAPGVGVAPGVGVAPGVGVAPGIGPGGVAA	496-526
64	GLAPGVGVAPGVGVAPGVGVAPGIGPGGVAAA	496-527
65	VAPGVGVAPGVGVAPGIGPGGV	503-524
66	VAPGVGVAPGVGVAPGIGPGGVAA	503-526

Table 1c continued..

67	APGVGVAPGVGVAPGIGPGGV	504-524
68	VGVAPGVGVAPGIGPGGVAA	507-526
69	GVAPGVGVAPGIGPGGV	508-524
70	GVAPGVGVAPGIGPGGVAAA	508-527
71	RAAAGLGAGIPGLGVGV	541-557
72	AGLGAGIPGLGV	544-555
73	GIPGLGVGVGVPGLGV	549-564
74	GVGVPGLGVGAGVPGLGVGA	556-575
75	GVPGLGVGAGVPGLGV	558-573
76	GVPGLGVGAGVPGLGVG	558-574
77	GVPGLGVGAGVPGLGVGA	558-575
78	GAGVPGLGVGAGVPGFGAVPGAL	565-587
79	GAGVPGFGAVPG	574-585
80	KYGAAVPGVLGGLGA	594-608
81	AVPGVLGGLGALGGV	598-612
82	VLGGLGALGGVGIPGGV	602-618
83	LGGLGALGGVGIPGGV	603-618
84	LGGLGALGGVGIPGGVVGAGPA	603-624
85	GGLGALGGVGIPGGVV	604-619
86	GGLGALGGVGIPGGVVGAGPA	604-624
87	GALGGVGIPGGVVGAGPA	607-624
88	LGGVGIPGGVVGAGPA	609-624
89	GGVGIPGGVVGAGPA	610-624
90	GLVGAAGLGGLGVG	640-653
91	GGLGVPGVGGLGGIPPAAA	653-671
92	GGLGVPGVGGLGGIPPAAAA	653-672
93	AAGLGGVLGGAGQFPLG	679-695
94	AGLGGVLGGAGQFPL	680-694
95	AGLGGVLGGAGQFPLG	680-695

Table 1c continued..

96	AGLGGVLGGAGQFPLGGV	680-607
97	GLGGVLGGAGQFPL	681-694
98	GLGGVLGGAGQFPLG	681-695
99	GLGGVLGGAGQFPLGGV	681-697
100	GLGGVLGGAGQFPLGGVAA	681-699
101	GGVLGGAGQFPLGGV	683-697
102	GGVAARPGF	695-703
103	GGVAARPGFGLSPIFPGGA	695-713
104	GVAARPGFGLSPI	696-708
105	GVAARPGFGLSPIFPGGA	696-713
106	VAARPGFGLSPI	697-708
107	VAARPGFGLSPIFPGGA	697-713
108	AARPGFGLSPI	698-708
109	AARPGFGLSPIF	698-709
110	AARPGFGLSPIFPG	698-711
111	AARPGFGLSPIFPGGA	698-713
112	ARPGFGLSPIFPG	699-711
113	RPGFGLSPI	700-708
114	RPGFGLSPIFPG	700-713
115	RPGFGLSPIFPGGA	700-713

The cleavage sites of the characterized peptides cover most of the hydrophobic domains in the precursor tropoelastin as shown in fig. 2A.

The proteomic analysis was also carried out with the peptide fractions below 10 kD obtained from the COPD lung ECM. This analysis also resulted in the identification of large numbers of the linear peptides: 150 peptides by HNE, 106 peptides by MMP12, and 126 peptides by PR3 digestions. The identities of peptides are shown in table 2a, 2b and 2c. Their cleavage sites are similar to that of normal lung with some additional cleavage sites spread into most of the hydrophobic domains in tropoelastin as shown in fig. 2B.

DISCUSSION

Effective degradation of lung elastic ECM by HNE, PR3 and MMP12

Proteolytic degradation of lung elastic ECM is a significant pathogenic process involved in the emphysema of COPD. As shown in fig. 1, three proteases, HNE, PR3 and MMP12 are particularly effective in the degradation of lung elastin matrix *in vitro* as indicated by the production of DES and IDS crosslinked peptides. It is likely that these three proteases also play a major role *in vivo*. The three proteases degrade the lung ECM into soluble peptide fragments with a large proportion of DES and IDS crosslinked peptides present in the fraction of molecular weights between 10–50 kD. Comparison of the proteolysis of the normal and COPD lung showed that the COPD lung produced decreased amounts of DES and IDS crosslinked peptides, which indicates a significant pathological degradation in the crosslinks of elastin matrix in the diseased lung. The photomicrograph of the COPD lung shows marked airspace enlargement, alveolar wall rupture and septal clubbing (Fig. 3).

Characterization of abundant linear peptide fragments from hydrophobic domains by LC-MS/MS proteomic analysis

Human tropoelastin has 36 domains which consists of alternating hydrophobic (rich in G, V, and L) and hydrophilic (rich in K and A) KA domains [24]. Elastin crosslinking occurs within the hydrophilic KA domains as a result of oxidative deamination of K residue by lysyl oxidase and subsequent intra- and intermolecular condensation to form bi-, tri- and tetrafunctional elastin crosslinks [25, 26]. The characterization of those crosslinked peptides cannot be achieved by the available database of proteomic analysis, but our comprehensive proteomic LC-MS/MS analysis of linear peptides can provide information on the crosslinking domains involved in tropoelastin. Our proteomic analysis results in the identification of large numbers of linear peptides derived from the hydrophobic domains of tropoelastin. Among the peptides, there are many free K residues present in the linear peptides as identified in table 1a, 1b, 1c, 2a, 2b, 2c, and in the cleavage sites (Fig. 2A and 2B). These free K residues present in the linear peptides are apparently not involved in elastin crosslinking.

Fig. 2A. Cleavage sites identified after digestion of normal lung ECM based on the sequence of tropoelastin isoform 9 (Swise Prot P15502-2). Cleavage sites are marked with triangles (HLM ▲ pink, MMP12 ▲ blue, Pr3 ▲ green) and sequence regions are labeled with solid lines.

Crosslinked domains and structure of tetrafunctional DES/IDS crosslinks

The structure of tetrafunctional DES/IDS crosslinks, a characteristic major elastin crosslinks, has been a subject of extensive investigations. Earlier peptide sequencing studies have shown that the tetrafunctional DES/IDS crosslinks were occurring through coupling between two peptide chains in poly alanine K

Fig. 2B. Cleavage sites identified after digestion of COPD lung ECM based on the sequence of tropoelastin isoform 9 (Swise Prot P15502-2). Cleavage sites are marked with triangles (HLM ▲ pink, MMP12 ▲ blue, Pr3 ▲ green) and sequence regions are labeled with solid lines.

domains [27-29]. A crosslinking structure by condensation between two pairs of K residues in two poly alanine helical hydrophilic KA domains, and condensation of -KAAK- (K at loci 379 and 382) at domain 19 and -KSAAK- (K at loci 529 and 533) at domain 25, to form a tetrafunctional DES/IDS crosslink, was proposed after complex amino acid sequencing and computer model emulation;

Table 2a. 150 peptides from NE digestion of COPD lung ECM (<10 kD).

No	Peptides	Location
1	FYPGAGLGAL	42-51
2	FYPGAGLGALGGG	42-54
3	ALGGGALGPGGKPLKPV	50-66
4	LGGGALGPGGKPL	51-63
5	GLAGAGLGAGLGAFPA	69-64
6	GLGAGLGAFPAV	74-85
7	VTFPGALVPGGV	85-96
8	VTFPGALVPGGVADAA	85-100
9	VTFPGALVPGGVADAAA	85-101
10	TFPGALVPGGVADAA	86-100
11	TFPGALVPGGVADAAA	86-101
12	FPGALVPGGV	87-96
13	FPGALVPGGVADAA	87-100
14	FPGALVPGGVADAAA	87-101
15	LVPGGVADAAA	91-101
16	KAGAGLGGVPGVGGLGV	107-123
17	GAGLGGVPGVGGLGV	109-123
18	AGLGGVPGVGGLGV	110-123
19	GLGGVPGVGGLG	111-122
20	GLGGVPGVGGLGV	111-123
21	GLGGVPGVGGLGVS	111-124
22	GLGGVPGVGGLGVSAGA	111-127
23	SAGAVVPQPGAGV	124-136
24	GLPGVYPGGVLPG	145-157
25	GVLPGARFPGV	153-163
26	ARFPGVGV	158-165
27	ARFPGVGVLPGVPT	158-171
28	VGVLPGVPT	163-171
29	GIPGVGPFGGPQPGVPL	188-204
30	VGPFGGPQ	192-199
31	VGPFGGPQPGVPL	192-204
32	PFGGPQPGVPL	194-204
33	KAPKLPG	209-215
34	GKLPYGYGPGGV	224-235
35	GKLPYGYGPGGVA	224-236
36	GKLPYGYGPGGVAGA	224-238
37	GAAGVLPGVGGAGVPGVPG	269-287
38	AGVLPGVGGAGV	271-282

Table 2a continued..

39	AGVLPGVGGAGVPGVPG	271-287
40	GVLPGVGGAGVPGVPG	272-287
41	GVLPGVGGAGVPGVPGAIPG	272-291
42	AIPGIGGIAGV	288-298
43	AAGLVPGGPGFGPGVV	319-334
44	AGLVPGGPGFGPG	320-332
45	AGLVPGGPGFGPGV	320-333
46	AGLVPGGPGFGPGVV	320-334
47	GLVPGGPGFGPGV	321-333
48	GLVPGGPGFGPGVV	321-334
49	GLVPGGPGFGPGVVG	321-335
50	PGGPGFGPGVV	324-334
51	VGVPGAGVPGVGV	334-346
52	VGVPGAGVPGVGVPG	334-348
53	VGVPGAGVPGVGVPGA	334-349
54	VGVPGAGVPGVGVPGAGIPV	334-353
55	GVPGAGVPGVGVP	335-347
56	GVPGAGVPGVGVPGA	335-349
57	GVPGAGVPGVGVPGAGIPV	335-353
58	AGVPGVGVPGAGIPV	339353
59	GVPGVGVPGAGIPV	340-353
60	AGIPVVPGAGIPG	349-361
61	VPGAGIPGAA	354-363
62	VPGAGIPGAAVPGVV	354-368
63	AGIPGAAVPGVV	357-368
64	GIPGAAVPGVV	358-368
65	AAVPGVVSPEAA	362-373
66	KYGARPGVGV	382-393
67	YGVGAGGFPGFGV	397-409
68	VGAGGFPGFGV	399-409
69	GAGGFPGF	400-407
70	GAGGFPGFG	400-408
71	GAGGFPGFGV	400-409
72	GAGGFPGFGVGV	400-411
73	AGGFPGFGV	401-409
74	GGFPGFGVGV	402-411
75	AGVPGVGGVPGVGGVPG	418-434
76	AGVPGVGGVPGVGGVPGVGI	418-437
77	GVPGVGGVPG	419-428

Table 2a continued..

78	GVPGVGGVPGVGGVPG	419-434
79	GVPGVGGVPGVGGVPGV	419-435
80	GVPGVGGVPGVGGVPGVGI	419-437
81	VGGVPGVGGVPGV	423-435
82	VGGVPGVGGVPGVG	423-436
83	VGGVPGVGGVPGVGI	423437
84	VGGVPGVGGVPGVGISPEAQAA	423-444
85	GGVPGVGGVPGVGI	424-437
86	GVPGVGGVPGVGI	425-437
87	QFGLVPGVG	470-478
88	QFGLVPGVGV	470-479
89	QFGLVPGVGVA	470-480
90	QFGLVPGVGVAPG	470-482
91	QFGLVPGVGVAPGV	470-483
92	QFGLVPGVGVAPGVGV	470-485
93	LVPGVGVAPGVGV	473-485
94	VGVAPGVGVAPGVGV	477-491
95	GVAPGVGVAPGVGV	478-491
96	GVAPGVGVAPGVGVAPG	478-494
97	APGVGVAPGV	480-489
98	APGVGVAPGVGVAPGV	480-495
99	APGVGVAPGVGL	486-497
100	APGVGVAPGVGLAPGVGV	486-503
101	GVAPGVGLAPGVGVAPG	490-506
102	VAPGVGLAPGVGV	491-503
103	APGVGLAPGVGV	492-503
104	APGVGLAPGVGVAPG	492-506
105	APGVGLAPGVGVAPGVGV	492-509
106	APGVGLAPGVGVAPGVGVAPGVGV	492-515
107	VGLAPGVGVAPGVGV	495-509
108	GLAPGVGVAPGVGV	496-509
109	GLAPGVGVAPGVGVAPGVGV	496-515
110	LAPGVGVAPGVGV	497-509
111	APGVGVAPGVGVAPGIGPGGV	504-524
112	APGVGVAPGIGPGGV	510-524

Table 2a continued..

113	APGVGVAPGIGPGGVA	510-525
114	APGVGVAPGIGPGGVAA	510-526
115	APGVGVAPGIGPGGVAAA	510-527
116	APGIGPGGVAAA	516-527
117	AAGLGAGIPGLGV	543-555
118	AGLGAGIPGLGV	544-555
119	AGLGAGIPGLGVGV	544-557
120	GLGAGIPGLGV	545-555
121	GLGAGIPGLGVGV	545-557
122	GIPGLGVGV	549-557
123	GVPGLGVGAGVPGLGV	558-573
124	LGVGAGVPGLGV	562-573
125	GAGVPGFGAVPG	574-585
126	GAGVPGFGAVPGAL	574-587
127	GAGVPGFGAVPGALA	574-588
128	GAGVPGFGAVPGALAA	574-589
129	AGVPGFGAVPGALA	575-588
130	GVPGFGAVPGALA	576-588
131	PGFGAVPGALA	578-588
132	AAVPGVLGGLGA	597-608
133	AVPGVLGGLGA	598-608
134	AVPGVLGGLGAL	598-609
135	AVPGVLGGLGALG	598-610
136	AVPGVLGGLGALGGV	598-612
137	VPGVLGGLGAL	599-609
138	PGVLGGLGALGGV	600-612
139	VLGGLGALGGV	602-612
140	LGGVGIPGGVV	609-619
141	GGLGVPGVGGL	653-663
142	GGLGVPGVGGLG	653-664
143	GGLGVPGVGGLGG	653-665
144	GGLGVPGVGGLGGIPPAAA	653-671
145	GGLGVPGVGGLGGIPPAAAA	653-672
146	GLGGVLGGAGQFPL	681-694
147	LGGAGQFPL	686-694
148	LGGAGQFPLGGV	686-697
149	GGVAARPGFGLSPI	695-708
150	AARPGFGLSPI	698-708

Table 2b. 106 peptides from MMP12 digestion of COPD lung ECM (<10 kD).

No	Peptides	Location
1	VFYPGAGLGA	41-50
2	VFYPGAGLGAL	41-51
3	LGALGGGALGPGGKPLKPVPGG	48-69
4	LGGGALGPGGKPLKPVPGG	51-69
5	LAGAGLGAGLGA	70-81
6	LAGAGLGAGLGAF	70-82
7	LAGAGLGAGLGAFP	70-83
8	LAGAGLGAGLGAFPA	70-84
9	LGAGLGAFPAV	75-85
10	LGAGLGAFPAVTFPGA	75-90
11	LGAFPAVTFPGA	79-90
12	AVTFPGALVPGG	84-95
13	AVTFPGALVPGGVADAAAA	84-102
14	LVPGGVADAAAA	91-102
15	AGAGLGGVPGVGG	108-120
16	LGVSAGAVVPQPGA	121-134
17	FAGIPGVGPF	186-195
18	FGGPQPGVPLGYP	195-207
19	IKAPKLPGG	208-216
20	IKAPKLPGGYGLP	208-220
21	YTTGKLPYGYGPGG	221-234
22	YTTGKLPYGYGPGGVAGAAGKAGYPTGTGVGPQA	221-254
23	YGPGGVAGAAGKAGYPTG	230-247
24	YGPGGVAGAAGKAGYPTGTGVGPQA	230-254
25	VAGAAGKAGYPTGTGVGPQA	235-254
26	VAGAAGKAGYPTGTGVGPQAAA	235-256
27	FGAGAAGVLPGVGG	266-279
28	AGVPGVPGAIPGIGG	280-294
29	IAGVGTPAA	295-303
30	IAGVGTPAAAAAAAAAAKA	295-313
31	YGAAAGLVPGGPGFG	316-330
32	YGAAAGLVPGGPGFGPGV	316-333
33	LVPGGPGFGPGV	322-333
34	LVPGGPGFGPGVVG	322-335
35	LVPGGPGFGPGVVGVPGA	322-339
36	YGARPGVGVGGIPTYG	383-398

Table 2b continued..

37	YGARPGVGVGGIPTYGVG	383-400
38	VGAGGFPGFG	399-408
39	VGAGGFPGFGVG	399-410
40	VGAGGFPGFGVGV	399-411
41	VGAGGFPGFGVGVG	399-412
42	VAGVPGVGGVPGVGGVPGVGISPEA	417-441
43	VGGVPGVGGVPGVGISPEA	423-441
44	VGGVPGVGISPEA	429441
45	AKAAAKAAQFG	462-472
46	FGLVPGVGVAPG	471-482
47	FGLVPGVGVAPGVG	471-484
48	FGLVPGVGVAPGVGVA	471-486
49	FGLVPGVGVAPGVGVAPG	471-488
50	FGLVPGVGVAPGVGVAPGVG	471-490
51	FGLVPGVGVAPGVGVAPGVGVAPG	471-494
52	VGVAPGVGLAPGVGVAPGVG	489-508
53	VGVAPGVGLAPGVGVAPGVGVAPGVGVAPGIGPGG	489-523
54	GVAPGVGLAPGVGVAPGVGVAPGVGVAPGIGPGG	490-523
55	VGLAPGVGVAPGVGVAPGVGVAPGIGPGG	495523
56	GLAPGVGVAPGVGVAPGVGVAPGIGPGG	496-523
57	LAPGVGVAPGVGVAPGVGVAPGIGPGG	497-523
58	VGVAPGVGVAPGVGVAPGIGPGG	501-523
59	GVAPGVGVAPGVGVAPGIGPGG	502-523
60	VGVAPGVGVAPGIGPGG	507-523
61	GVAPGVGVAPGIGPGG	508-508
62	LGAGIPGLGV	546-555
63	LGAGIPGLGVGVGVPG	546-561
64	LGVGVGVPGLG	553-563
65	VGVGVPGLGVGAGVPGLG	555-572
66	VGAGVPGLGVGA	564-575
67	VGAGVPGLGVGAGVPGFGAVPGA	564-586
68	AGVPGLGVGAGVPGFGAVPGA	566-586

Table 2b continued..

69	VGAGVPGFG	573-581
70	VGAGVPGFGAVPGA	573-586
71	YGAAVPGVL	595-603
72	YGAAVPGVLGG	595-605
73	YGAAVPGVLGGLG	595-607
74	YGAAVPGVLGGLGA	595-608
75	LGGLGALGGVGIPGG	603-617
76	LGALGGVGIPGG	606-617
77	LGALGGVGIPGGVVGAGPAA	606-625
78	ALGGVGIPGG	608-617
79	LGGVGIPGGVVG	609-620
80	LGGVGIPGGVVGAGPAA	609-625
81	VVGAGPAAAAAAAKAAA	618-634
82	LVGAAGLGGLGV	641-652
83	LVGAAGLGGLGVG	641-653
84	LVGAAGLGGLGVGG	641-654
85	VGAAGLGGLGVGG	642-654
86	LGGLGVGGLGVPGVG	647-661
87	LGGLGVGGLGVPGVGG	647-662
88	LGGLGVGGLGVPGVGGLGGIPPAAA	647-671
89	LGVGGLGVPGVGG	650-662
90	VGGLGVPGVGG	652-662
91	LGVPGVGGLGGIPPAA	655-670
92	LGVPGVGGLGGIPPAAA	655-671
93	LGGIPPAAA	663-671
94	LGGVLGGAGQF	682-692
95	LGGVLGGAGQFPL	682-694
96	LGGVLGGAGQFPLG	682-695
97	LGGVLGGAGQFPLGG	682-696
98	LGGVLGGAGQFPLGGVAARPG	682702
99	VLGGAGQFPLGG	685-696
100	LGGVAARPGFGL	694705
101	LGGVAARPGFGLSP	694-707
102	LGGVAARPGFGLSPIFPGG	694-712
103	GVAARPGFGL	696-705
104	GVAARPGFGLSPIFPGG	696-712
105	VAARPGFGLSPIFPG	697-711
106	VAARPGFGLSPIFPGGA	697-713

Table 2c. 126 peptides from PR3 digestion of COPD lung ECM (<10 kD).

No	**Peptides**	**Location**
1	LGGGALGPGGKPLKPVPGGL	51-70
2	LGGGALGPGGKPLKPVPGGLA	51-71
3	LGGGALGPGGKPLKPVPGGLAGA	51-73
4	LGGGALGPGGKPLKPVPGGLAGAGL	51-75
5	LGGGALGPGGKPLKPVPGGLAGAGLGA	51-77
6	GGGALGPGGKPLKPVPGGL	52-70
7	GLGAGLGAFPAV	74-85
8	VTFPGALVPGGV	85-96
9	KAGAGLGGVPGVGGL	107-121
10	KAGAGLGGVPGVGGLGV	107-123
11	GAGLGGVPGVGGLGV	109-123
12	SAGAVVPQPGAGVKPGKVPGV	124-144
13	GLPGVYPGGVLPGA	145-158
14	VYPGGVLPGARFPGV	149-163
15	ARFPGVGV	158-165
16	ARFPGVGVLPGVPT	158-171
17	ARFPGVGVLPGVPTG	158-172
18	RFPGVGVLPGVPT	159-171
19	KAPKLPGGY	209-217
20	GYGPGGVAGAAGKA	229-242
21	AGKAGYPTGTGVGPQ	239-253
22	AKFGAGAAGVLPGVGGA	264-280
23	VGGAGVPGVPGAIPGIGGIAGV	277-298
24	GGAGVPGVPGAIPG	278-291
25	GGAGVPGVPGAIPGIGGI	278-295
26	GGAGVPGVPGAIPGIGGIAGVGTPA	278-302
27	GVPGVPGAIPGIGGIAGVGTPA	281-302
28	AIPGIGGIAGVGTPA	288-302
29	GAAAGLVPGGPGFGPGVV	317334
30	AAGLVPGGPGFGPGVV	319-334
31	AGLVPGGPGFGPGV	320-333
32	GLVPGGPGFGPGVVGVPGA	321-339
33	GLVPGGPGFGPGVVGVPGAGVPG	321343
34	GLVPGGPGFGPGVVGVPGAGVPGV	321-344

Table 2c continued..

35	LVPGGPGFGPGV	322-333
36	LVPGGPGFGPGVV	322-334
37	GPGVVGVPGAGVPGVGVPGAGIPV	330-353
38	VGVPGAGVPGVGVPGAGIPV	334-353
39	VGVPGAGVPGVGVPGAGIPVVPGA	334-357
40	VGVPGAGVPGVGVPGAGIPVVPGAGIPGA	334-362
41	GVPGAGVPGVGVPGAGIPV	335-353
42	GVPGAGVPGVGVPGAGIPVVPGA	335-357
43	KYGARPGVGVGGIPT	382-396
44	GARPGVGVGGIPT	384-396
45	GARPGVGVGGIPTY	384397
46	ARPGVGVGGIPT	385-396
47	AGVPGVGGVPGVGGVPGVGISPEAQ	418-442
48	GVPGVGGVPGVGGVPGVGISPEAQ	419-442
49	AKYGVGTPA	450-458
50	AQFGLVPGVGVAPGV	469-483
51	AQFGLVPGVGVAPGVGV	469-485
52	AQFGLVPGVGVAPGVGVAPGV	469-489
53	AQFGLVPGVGVAPGVGVAPGVGVAPGV	469-395
54	QFGLVPGVGVAPGVGV	470-485
55	QFGLVPGVGVAPGVGVA	470-486
56	QFGLVPGVGVAPGVGVAPGV	470-489
57	QFGLVPGVGVAPGVGVAPGVG	470-490
58	QFGLVPGVGVAPGVGVAPGVGVAPG	470-494
59	QFGLVPGVGVAPGVGVAPGVGVAPGV	470-495
60	GLVPGVGVAPGVGV	472-485
61	GLVPGVGVAPGVGVAPGVGVAPG	472-494
62	GLVPGVGVAPGVGVAPGVGVAPGV	472-495
63	VGVAPGVGVAPGVGVAPGV	477-495
64	GVAPGVGVAPGVGLAPGVGVAPG	484506
65	GVAPGVGVAPGVGLAPGVGVAPGVGVAPGV	484-513

Table 2c continued..

66	VGLAPGVGVAPGVGVAPGVGVAPG	495-518
67	GLAPGVGVAPGVGV	496-509
68	GLAPGVGVAPGVGVAPGV	496-513
69	GLAPGVGVAPGVGVAPGVGV	496-515
70	GLAPGVGVAPGVGVAPGVGVAPGIG	496-520
71	GLAPGVGVAPGVGVAPGVGVAPGIGPGGV	496-524
72	GLAPGVGVAPGVGVAPGVGVAPGIGPGGVA	496-525
73	GLAPGVGVAPGVGVAPGVGVAPGIGPGGVAA	496-526
74	GLAPGVGVAPGVGVAPGVGVAPGIGPGGVAA	496-527
75	GVAPGVGVAPGVGVAPGIGPGGV	502-524
76	GVAPGVGVAPGVGVAPGIGPGGVAA	502-526
77	APGVGVAPGVGVAPGIGPGGVAAA	504-527
78	VGVAPGVGVAPGIGPGGVA	507-525
79	VGVAPGVGVAPGIGPGGVAA	507-526
80	VGVAPGVGVAPGIGPGGVAAA	507-527
81	GVAPGVGVAPGIGPGGVAAA	508-527
82	VAPGVGVAPGIGPGGVAA	509-526
83	GVAPGIGPGGV	514-524
84	AGLGAGIPGLGV	544-555
85	AGLGAGIPGLGVGV	544-557
86	GVGVPGLGVGAGVPGL	556-571
87	GVPGLGVGAGVPGL	558-571
88	GVPGLGVGAGVPGLGV	558-573
89	GVPGLGVGAGVPGLGVG	558-574
90	GVPGLGVGAGVPGLGVGA	558-575
91	GAGVPGLGVGAGVPGF	565-580
92	GAGVPGLGVGAGVPGFGAVPGAL	565-587
93	GVPGLGVGAGVPGFGAVPG	567-585
94	AKYGAAVPGVL	593-603
95	KYGAAVPGVL	594-603
96	KYGAAVPGVLGGLGA	594-608
97	GAAVPGVLGGLGAL	596-609
98	LGGLGALGGVGIPGGV	603-618

Table 2c continued..

99	GGLGALGGVGIPGGVV	604-619
100	GGLGALGGVGIPGGVVGAGPA	604624
101	LGGVGIPGGVVGAGPA	609-624
102	QFGLVGAAGLGGLGV	638-652
103	GLVGAAGLGGLGV	640-652
104	AGLGGLGVGGLGVPGV	645-660
105	GGLGVPGVGGLGGIPPA	653-669
106	GGLGVPGVGGLGGIPPAAA	653-671
107	GGLGVPGVGGLGGIPPAAAA	653-72
108	KYGAAGLGGVLGGAGQ	676-691
109	GAAGLGGVLGGAGQFPL	678-694
110	AAGLGGVLGGAGQFPL	679-694
111	AAGLGGVLGGAGQFPLGGV	679-697
112	AGLGGVLGGAGQFPLG	680-695
113	AGLGGVLGGAGQFPLGGV	680-697
114	GLGGVLGGAGQFPL	681-694
115	GLGGVLGGAGQFPLG	681-695
116	GGVLGGAGQFPL	683-694
117	VLGGAGQFPLGGV	685-697
118	LGGAGQFPL	686-694
119	GGVAARPGFGL	695-705
120	GGVAARPGFGLSPI	695-708
121	GVAARPGFGL	696-705
122	GVAARPGFGLSPI	696-708
123	VAARPGFGLSPI	697-708
124	AARPGFGLSPIFPG	698-711
125	AARPGFGLSPIFPGGA	698-713
126	ARPGFGLSPIFPG	699-711

however, there is no easy way to confirm the structure [30]. There are a total of 35 K residues in the elastin precursor tropoelastin before crosslink. In this study, our extended *in vitro* proteolysis of the lung ECM resulted in the identification of as much as 18 of the free K residues in linear peptides which are apparently not involved in crosslinking formation. The remaining 17 of the K residues in tropoelastin could involve in the crosslinking of elastin. Among them the two polyalanine KA domains 19 and 25 are identified as most likely involved in the formation of a tetrafunctional DES/IDS crosslink. However, our results further indicate that the K residue at the locus 382 could not involve in the crosslink, because the proteolysis of both normal and COPD lungs cleave the K residue at locus 382 (Fig. 2A and Fig. 2B) to produce a linear peptide KYGARPGVGV (peptide no.22 in table 1a and peptide no. 66 in table 2a). Therefore, we propose that a tetrafunctional DES/IDS crosslink must be formed at the preceding poly alanine loci, between KAAAK (K at loci 375 and 379) at domain 19 and KSAAK (K at loci 529 and 533) at domain 25.

DES/IDS crosslink peptides represent the major crosslinking biomarkers for elastin matrix degradation processes in many diseases. The crosslink peptides may contribute to the backbone structure of mature elastin and provide physical recoil to distorting forces and contribute to normal physiological function, yet their molecular structures remain to be elucidated. Recently a new proteomic software named PolyLynx to analyze elastin crosslink peptides has been developed [31-33]; however, the characterization of tetrafunctional DES/IDS crosslink peptides from digests of mature elastin remains a challenge. Further study of mass spectrometric fragmentation on a structurally defined tetrafunctional DES/IDS crosslinked peptide model will be an effective approach. Our laboratories have been engaging in various chemical syntheses of DES and IDS molecules [34-37]. The chemical synthesis of the DES/IDS crosslinked peptide model by condensation of KAAAK (K at loci 375 and 379) and KSAAK (K at loci 529 and 533) that we have proposed is under progress.

Proteolysis of normal and COPD lung

We compared *in vitro* proteolysis of a normal lung and a lung from a COPD patient. The proteolysis of COPD lung showed that the three proteases HNE, MMP12 and PR3 are the most effective toward elastin matrix degradation. The proteolysis of the COPD lung produced decreased amount of DES/IDS crosslink peptides compared to that of the normal lung, which indicated significant pathological degradation of the crosslinks had occurred within the elastin matrix. The proteolysis of COPD lung involved more cleavage sites than that of normal lung (compare Fig 2A and Fig. 2B). More proteolysis sites observed in the COPD lung might be due to the increase in the accessibility of proteolytic

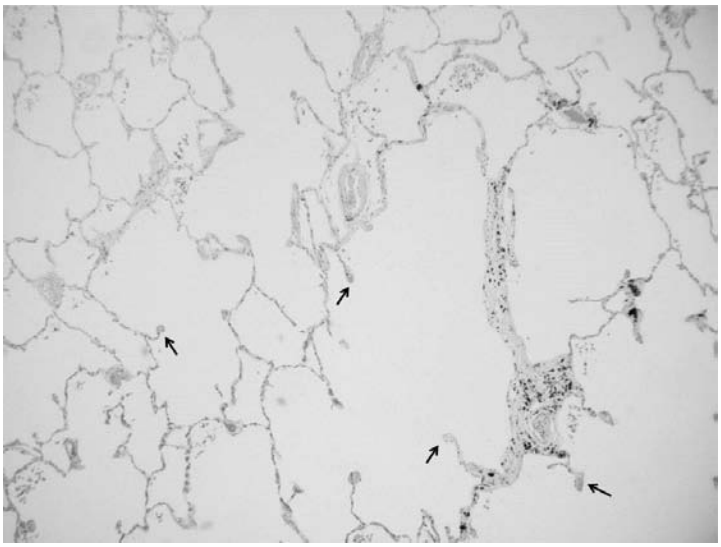

Fig. 3. Photomicrograph of emphysematous COPD Lung. Lung tissue from the COPD patient showing marked airspace enlargement with alveolar wall rupture and septal clubbing (arrows). Scattered deposits of anthracotic pigment with associated fibrosis are also present, consistent with a history of smoking.

enzymes as the result of loss in the crosslinks and altered configuration of the matrix (as indicated in fig. 3). This finding could be a basis for progression of lung tissue breakdown once COPD is initiated and reflects the clinical progression of COPD.

CONCLUSION

We compared *in vitro* proteolysis of a normal and a COPD lung elastin matrix. The proteolysis showed the three proteases HNE, MMP12 and PR3 are the most effective toward elastin matrix degradation, which may also occur *in vivo* during COPD. The LC-MS/MS analysis of the proteolytic peptides identified a large number of linear peptides cleaved at hydrophobic domains of tropoelastin. Most of the tetrafunctional DES/IDS crosslink peptides were present in the 10 kD to 50 kD fraction. The proteolysis of the COPD lung that produces decreased amount of DES/IDS crosslink peptides with increased numbers of cleavage sites indicated the loss of the crosslinks and structural integrity in COPD lung. The finding might indicate the progression of lung tissue breakdown once COPD is initiated and reflects the clinical progression of COPD.

Our proteomic LC-MS/MS analysis indicates that two alanine-rich lysine peptide chains at the domains 19 and 25 of tropoelastin are most likely involved in the crosslink formation. A tetrafunctional DES/IDS crosslink by condensation of KAAAK (K at loci 375 and 379) and KSAAK (K at 529 and 533) is proposed. The chemical synthesis of this DES/IDS crosslinking model compound and its LC-MS/MS study are under investigation.

FUNDING AND ACKNOWLEDGMENTS

This work was supported by funds from a Boehringer Ingelheim investigator grant, the James P. Mara Center for Lung Disease (New York, NY, USA), the Flight Attendants Medical Research Institute (Miami, FL, USA), the Charles A. Mastronardi Foundation (Wilmington DE, USA), the Ned Doyle Foundation (New York) and the Alpha One Foundation (Miami), and also by funds from Ethel Kennedy, John Kennedy and Judith Sulzberger (New York). LC-MS proteomics work was supported by NIH/NINDS (P30 NS061777) and NIH NCRR (S10 RR022415).

CONFLICT OF INTEREST STATEMENT

The authors report no conflicts of interest. The authors alone are responsible for the content and writing of the paper.

REFERENCES

1. Sandberg, L. B. and Soskel, L. L. G. 1981, N. Engl. J. Med., 304, 566.

2. Rosenbloom, J. 1982, Connect Tissue Res., 10, 73.
3. Wright, R. R. 1961, Am. J. Pathol., 39, 355.
4. Chrzanowski, P., Keller, S., Cerreta, J., Mandl, I. and Turino, G. M. 1980, Am. J. Med., 69, 351.
5. Barnes, P. J. 2000, New Eng. J. Med., 343, 269.
6. Thomas, J., Eldson, D. F. and Patridge, S. M. 1963, Nature, 200, 651.
7. Shimada, W., Bowman, N. R. and Anwar, R. A. 1969, Biochem. Biophys. Res. Commun., 37, 191.
8. Akagawa, M. and Suyama, K. 2000, Connect. Tissue Res., 41, 131.
9. Suzuki, R., Yanuma, H., Hayashi, T., Yamada, H. and Usuki, T. 2015, Tetrahedron, 71, 1851.
10. Ma, S., Turino, G. M., Hayashi, T., Yanuma, H., Usuki, T. and Lin, Y. Y. 2013, Anal. Biochem., 440, 158.
11. Ma, S., Lieberman, S., Turino, G. M. and Lin, Y. Y. 2003, Proc. Nat. Acad. Sci., 1000, 12941.
12. Ma, S., Turino, G. M. and Lin, Y. Y. 2011, J. Chrom. B, 879, 1893.
13. Ma S., Lin, Y. Y. and Turino, G. M. 2007, Chest, 131, 1363.
14. Ma, S., Lin, Y. Y. and Turino, G. M. 2009, Respir. Res., 10, 12.
15. Ma, S., Lin, Y. Y., He, J., Rouhani, F. N., Brandly, M. and Turino, G. M. 2013, COPD, 10, 473.
16. Slowik, N., Ma, S., He, J., Lin, Y. Y., Soldin, O. P., Robbins, R. and Turino, G. M. 2011, Chest, 40, 943.
17. Senior, R. M., Griffen, G. L. and Mecham, R. P. 1980, J. Clin. Invest., 66, 859.
18. Houghton, A. M., Quintero, P. A., Perkins, D. L., Kobayashi, D. K., Kelly, D. G., Marconcini, L. A., Mecham, R. P., Senior, R. M. and Shapiro, S. D. 2006, J. Clin. Invest., 116, 753.
19. Lee, S. H., Goswami, S., Grudo, A., Song, L. G., Bandi, V., Goodnigt-white, S., Green, L., Hacken-Bitar, J., Huh, J., Bakaeen, F., Coxson, H. O., Cogswell, S., Storness-Bliss, C., Corry, D. B. and Kheradmand, F. 2007, Nat. Med., 13, 567.
20. Cosio, S. G., Saetta, M. and Agusti, A. 2009, N. Eng. J. Med., 360, 2445.
21. Bhavani, S., Tsai, C. L., Perusich, S., Hesselbacher, S., Coxson, H., Pandit, L., Corry, D. B. and Kheradmand, F. 2015, Am. J. Resir. Crit. Care Med., 192, 1171.
22. He, J., Turino, G. M. and Lin, Y. Y. 2010, Exper. Lung Res., 36, 548.
23. Shapiro, S. D. 2002, Biochem. Soc. Trans, 30, 98.
24. Vrhovski, B. and Weis, A. S. 1998, Eur. J. Biochem., 258, 1.
25. Mecham, R. P. and Davis, E. C. 1994, Extracellular Matrix Assembly and Structure (P. D. Yurchenko, P. E. Berk, R. P. Mecham, (Eds.)), Academic Press, Sandiego, 281.
26. Akagawa, M. and Suyama, K. 2000, Connect Tissue Res., 41, 131.
27. Garber, G. E. and Anwer, R. A. 1974 J. Biol. Chem., 249, 5200.
28. Foster, J. A., Rubin, L., Kagan, H. M., Franzblau, C., Bruenger, E. and Sandberg, L. B. 1974, J. Biol. Chem., 249, 6191.
29. Baig, K. M., Vlaovic, M. and Anwer, R. A. 1980, Biochem. J., 185, 611.
30. Brown-Augsburger, P., Tisdale, C., Broekelmann, T., Sloan, C. and Mecham, R. P. 1995, J. Bio. Chem., 270, 17778.
31. Heinz, A., Ruttkies, C. K. H., Jahreis, G., Schrader, U., Wichapong, K., Sippl, W., Keeley, F. W., Newbert, R. H. and Schmelzer, C. E. 2013, Biophim. Biophy. Acta, 1830, 2994.
32. Heinz, A., Schrader, C. U., Stephanie, B., Keeley, F. W., Mithieux, S. M., Weis, A. S., Neubert, R. H. H. and Schmelzer, C. E. H. 2014, Matrix Biology, 38, 12.
33. Schrader, C. U., Heinz, A., Majovsky, P. and Schmelzer, C. E. H. 2015, J. Am. Soc. Mass Spectrom., 26, 762.
34. Usuki, T, Yamada, H., Hayashi, T., Yanuma, H., Koseki, Y., Suzuki, N., Masuyama, Y. and Lin, Y. Y. 2012, Chem. Comm., 48, 3233.
35. Yanuma, H. and Usuki, T. 2012, Tetrahedron Lett., 53, 5920.
36. Usuki, T., Sugimura, T., Komatsu, A. and Kosei, Y. 2014, Org. Lett., 16, 1672.
37. Koseki, Y., Sugimura, T., Ogawa, K., Suzuki, R., Yamada, H., Suzuki, N., Masuyama, Y., Lin, Y. Y. and Usuki, T., 2015, Eur. J. Org. Chem., 18, 4024.